April 2001

ELSEVIER

Materials Letters 48 (2001) 253–257

MATERIALS LETTERS

www.elsevier.com/locate/matlet

Lattice parameters of thoria–yttria solid solutions

I.C. Cosentino, R. Muccillo *

Instituto de Pesquisas Energéticas e Nucleares, Comissão Nacional de Energia Nuclear, C.P. 11049, Pinheiros, Sao Paulo, S.P., 05422-970, Brazil

Received 11 September 2000; accepted 26 September 2000

Abstract

ThO_2:x mol% Y_2O_3 ($x = 0$, 3, 6, 9 and 12) ceramic powders have been prepared by the citrate technique. Dense specimens have been obtained after pressing and sintering at 1550°C/2 h. X-ray diffraction measurements were performed in the sintered pellets for structural phase analysis and lattice parameter determination. The experimental results suggest that an empirical equation, similar to the equation proposed for zirconia–yttria ceramics, is valid for thoria–yttria solid solutions.

PACS: 61.10.N; 77.84
Keywords: Solid electrolytes; Thoria–yttria; Lattice parameter

1. Introduction

Thorium oxide, like other oxides of tetravalent cations (zirconium oxide, cerium oxide) is a material with predominant electrical conduction via O^{2-} ions [1]. A wide range of applications of these materials, after forming solid solutions with oxides of lower valent cations, is found in modern technology. They are used in oxygen sensors in the steel and in the automotive industries, and in solid oxide fuel cells [2,3]. The role played by the dopants with lower valence ($2+$ and $3+$) than the host ($4+$) is the introduction of oxygen vacancies in the lattice, required for charge neutrality, these vacancies being responsible for the observed high ionic conductivity in these systems. The ionic conductivity of fluorite type oxides, e.g., doped thoria and doped zirconia, depends on the dopant kind and concentration. Maximum conductivity is achieved with dopants having ionic radius close to the ionic radius of the host ion, i.e., the lower is the lattice contraction or expansion, the higher is the ionic conductivity [4]. The effect of dopants on the lattice parameters of the cubic fluorite structure phase is thus important in the study of oxygen-ion conductors [4]. Several equations have been proposed for the dependence of the lattice parameter of fluorite structure MO_2 oxide solid solutions on dopant concentration [4–8]. For the determination of lattice parameters in MO_2–R_2O_3 systems (M = Zr, Hf, Th and R = La, Pr, Nd, Sm, Sc, Y, Ln) as a function of dopant content, the dopant–host radius difference and the contraction of the lattice

* Corresponding author. Tel.: +55-118169343; fax: +55-118169370.
E-mail address: muccillo@usp.br (R. Muccillo).

00167-577X/01/$ - see front matter
PII: S0167-577X(00)00311-6

due to the creation of oxygen-ion vacancies was considered [8]. The differences between calculated and experimentally determined lattice parameters were lower than 0.03 Å for Zr and Hf systems. For Th systems, on the other hand, the calculations did not yield good results. Based on the effect of the solute ion size and oxygen-ion vacancies on the geometry of the fluorite unit cell, empirical equations have been proposed for the observed changes in the lattice parameters of MO_2 fluorite-type oxides (M = Hf, Zr, Ce, Th, U) due to formation of solid solutions [4]. A critical ionic radius is defined for each system as the hypothetical radius of the dopant whose substitution for the host cation causes neither expansion nor contraction of the fluorite lattice; the closer the dopant ionic radius is to the critical ionic radius, the higher is the ionic conductivity [4]. The changes of lattice parameters of cubic solid solutions, particularly of the ZrO_2–Y_2O_3 system, have been estimated assuming a spherical ion packing [6]. The experimental determination of lattice parameters by X-ray diffraction measurements in ZrO_2–Y_2O_3 single crystals in the 2–5 mol% Y_2O_3 range gave support to these estimations. That model was considered correct for ZrO_2 and HfO_2 systems but not for ThO_2, CeO_2 and UO_2 systems. The difference is that these systems can retain the fluorite structure at room temperature without doping, while the other two systems (ZrO_2 and HfO_2) require aliovalent doping for that purpose [5]. Moreover, oxygen-ion vacancy formation upon doping is not taken into consideration in that model. More recently, an ion packing model was proposed based on cluster of defects in zirconia solid solutions [7].

Thorium oxide is known as one of the structurally more stable oxides. Its structure is cubic fluorite up to the melting point at approximately 3300°C. Yttrium oxide crystallizes with the Tl_2O_3-type, the common structure to the majority of the rare earth oxides [10]. That structure derives from the cubic fluorite structure by an ordered omission of one quarter of the anions and a slight rearrangement of the ions. Based on the similarity of the structure, extensive solid solution can be obtained in the ThO_2–Y_2O_3 system [10].

For the evaluation of the experimentally determined lattice parameters of thoria–yttria specimens, two models previously proposed have been used in this paper [6,14]. The first one, proposed for ZrO_2:Y_2O_3 solid solutions for yttria concentration up to 12 mol% presented the following equation:

$$d_0 = 0.1A\left\{R_{\mathrm{Th}} + R_0 + \frac{\sum_k P_k M_k \Delta R_k}{100 + \sum_k M_k (P_k - 1)}\right\}$$

R_0 is the O^{2-} ionic radius, R_k the ionic radius of the kth doping element, P_k the number of ions by unit cell of the kth doping element, A a parameter related to the structure geometry.

Considering that yttrium is the doping element, the above equation simplifies to

$$d_0 = 0.1A\left\{R_{\mathrm{Th}} + R_0 + \frac{PM\Delta R}{100 + M(P - 1)}\right\}$$

Using the Pauling ionic radii for Th^{4+} ($R_{\mathrm{Th}} = 1.02$ Å), for Y^{3+} ($R_{\mathrm{Y}} = 0.93$ Å) and for O^{2-} ($R_{\mathrm{O}} = 1.40$ Å), $A = 4/\sqrt{3}$ for the cubic fluorite structure, and $P = 2$ for the yttrium oxide, the following equation is obtained:

$$d_0 = 0.23094\left\{2.42 - \frac{0.18M}{100 + M}\right\}$$

That equation is the first one used for calculating the lattice parameter of the thoria–yttria specimens prepared in this work.

The second model is the one recently proposed for determining lattice parameters in fluorite (MO_2) and C-type ($MO_{1.5}$) solid solutions [14]. According to the authors, it can be applied in the full composition range and it also shows that for relatively large M^{4+} substituting cations (Th, Ce), there is a positive (convex) deviation from the Vegard's law; for M^{4+} relatively small (Zr, Hf) cation ionic radii, on the other hand, the deviation is (concave) negative. The basic equation to evaluate the lattice parameter a_0 of the $M_{1-y}M'_yO_{2-y/2}$ ($0 < y < 1$) solid solution is:

$$a_0(y) = (1 - y) f_{\mathrm{F}} + y f_{\mathrm{C}}$$

y is the molar fraction of the cubic oxide, f_{F} (r_{C}) the curve fitting of the lattice parameter of the fluorite-type oxides (MO_2) as a function of the corresponding (M^{4+}) cationic radius, and f_{C} (r_{C}) the curve fitting using lattice parameter values for cubic ($MO_{1.5}$) oxides as a function of the corresponding (M^{3+}) cationic radius.

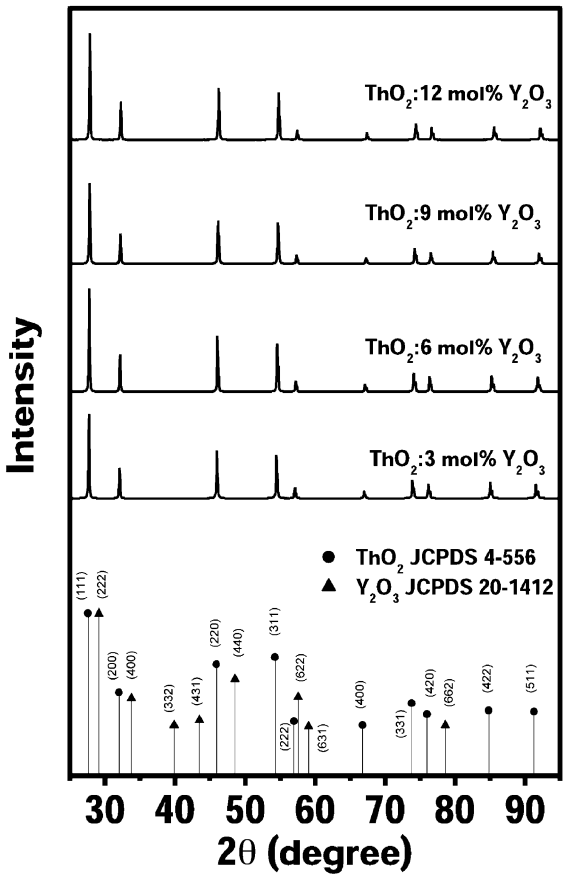

Fig. 1. X-ray diffraction patterns of ThO_2:m mol% Y_2O_3 ($m = 3$, 6, 9 and 12) sintered pellets. Bottom: main X-ray diffraction lines for ThO_2 and Y_2O_3 from JCPDS files.

The fitting equations leading to f_F and f_C values depend on r_C, the average cationic radius of the solid solution, determined at the average oxygen coordination number of $(8 - 2y)$ at composition y:

$$r_C = (1 - y) \cdot r_{M^{4+}} + y \cdot r_{M^{3+}}$$

The ionic radii $r_{M^{4+}}$ and $r_{M^{3+}}$ were evaluated from the Shannon's ionic radii table [9].

This work presents the experimental lattice parameters determined on carefully prepared ThO_2:m mol% Y_2O_3 ($m = 0$, 3, 6, 9, 12) specimens and also the fitting of these parameters as a function of yttria concentration using two proposed models.

2. Experimental

Thoria–yttria reactive (high surface area) powders have been prepared according to the citrate technique [11–13] for yttria contents 3, 6, 9 and 12 mol%. The powders were pressed to pellets and sintered at 1550°C/2 h. Finishing of the pellet surfaces has been achieved by polishing. X-ray diffraction analysis has been performed in the parallel pellet surfaces in the 25–95° 2Θ range (0.02° angle step size, 5 s time per step). Bruker-AXS D8 Advance and Philips 3710 diffractometers were used at 40 kV and 40 mA.

3. Results and discussion

The X-ray diffraction patterns of the sintered ThO_2–Y_2O_3 specimens are shown in Fig. 1. The diffraction lines of pure ThO_2 and Y_2O_3 from JCPDS files are also shown. The diffraction patterns of the specimens correspond to that of pure ThO_2, no diffraction lines of Y_2O_3 being detected. As far as X-ray diffraction experiments are concerned, thoria–yttria solid solution has been attained in all doped specimens. Impedance spectroscopy experiments on these yttria-doped specimens described elsewhere [12,13] provided further evidence of solid solution formation.

The lattice parameters were determined for each composition after indexing all diffraction lines. Table 1 shows these values.

There is a decrease in the lattice parameter values for increasing Y_2O_3 addition. The same behavior has already been reported for thoria–yttria ceramics for

Table 1
Lattice parameter values for sintered. ThO_2:x mol% Y_2O_3 ($x = 0$, 3, 6, 9 and 12)

Nominal composition	Lattice parameter (Å)
ThO_2 [a]	5.5921
ThO_2:3 mol% Y_2O_3	5.5845
ThO_2:6 mol% Y_2O_3	5.5725
ThO_2:9 mol% Y_2O_3	5.5626
ThO_2:12 mol% Y_2O_3	5.5543

[a] JCPDS file 42-1462.

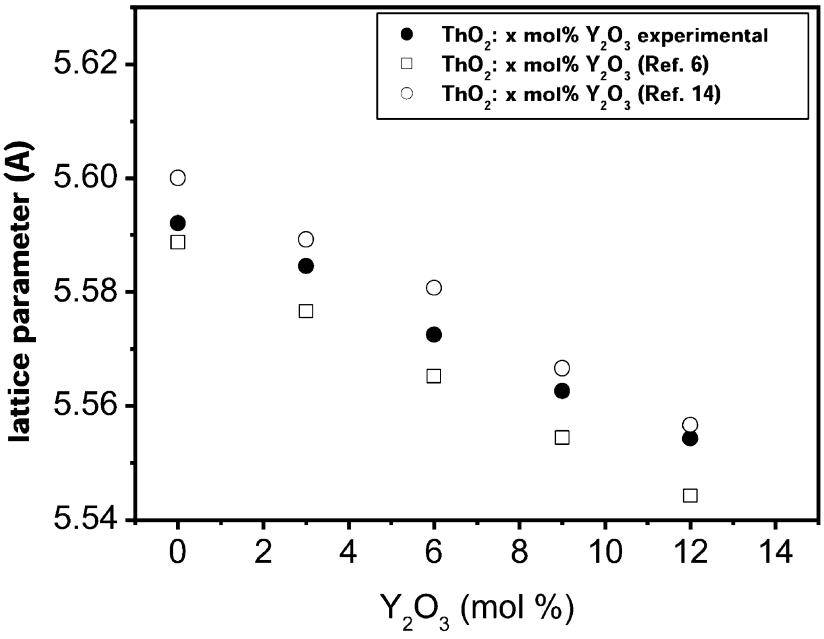

Fig. 2. Lattice parameter of ThO_2:*m* mol% Y_2O_3 (*m* = 0, 3, 6, 9 and 12) sintered pellets as a function of Y_2O_3 content: ●—experimental, ○—according to model 1 Ref. [6], □—model 2 Ref. [14].

yttria concentrations in the 0–33% range [10]. The substitution of Y^{3+} for Th^{4+} in the crystal lattice promotes local contraction due to the difference in ionic radius (1.02 Å for Th^{4+} and 0.93 Å for Y^{3+}). An opposite behavior is found in zirconia–yttria systems, the lattice parameter increasing for increasing yttria content due to a local expansion of the crystal lattice (the ionic radius of Zr^{4+} is 0.80 Å).

Fig. 2 shows the dependence of the lattice parameter of ThO_2–Y_2O_3 on the Y_2O_3 content. The theoretical values of the lattice parameter, determined using the equation corresponding to the first model, are plotted for comparison with the experimentally determined values. A good agreement is found. As expected, the values determined experimentally by X-ray diffraction are higher than the calculated ones. Even though there are no Y_2O_3 diffraction lines in the X-ray diffraction patterns, probably not all added yttrium ions are soluble in the ThO_2 matrix. The larger the Y_2O_3 content added to the ThO_2 matrix, the larger the difference between the experimental and the calculated lattice parameters.

In the same figure, the values determined using the second model, proposed recently by Otobe and Nakamura, are also shown. A good agreement is also found. The main difference between both models is that the first shows large deviation for increasing yttria content, while for the second the deviation is at low yttria concentrations.

4. Conclusions

One model developed for the dependence of the lattice parameter on the dopant content of zirconia ceramics was successfully applied to thoria–yttria ceramic solid electrolytes in the 0–12 mol% yttria composition range. The model, proposed by Ingel and Lewis, fits the experimentally determined decrease of the lattice parameter of thoria–yttria for increasing yttria content in that range. In this case, the larger the dopant concentration, the larger the deviation between experimental and calculated lattice parameters. Another model, recently proposed by Otobe and Nakamura, also fits the experimental data. In this case, the larger the dopant concentration, the smaller the deviation.

Acknowledgements

To the Brazilian Nuclear Energy Commission, FAPESP, PRONEX, CAPES and CNPq.

References

[1] R.M. Dell, A. Hooper, in: P. Hagenmuller, W. Van Gool (Eds.), Solid Electrolytes—General Principles, Characterization, Materials, Applications, Academic Press, New York, 1978, 291.
[2] A.K. Mehrotra, H.S. Maiti, E.C. Subbarao, Mater. Res. Bull 8 (1973) 899.
[3] in: E.C. Subbarao (Ed.), Solid Electrolytes and their Applications, Plenum, New York, 1980.
[4] D.-J. Kim, J. Am. Ceram. Soc. 72 (1989) 1415.
[5] V.I. Aleksandrov, G.E. Val'yano, B.V. Lukin, V.V. Osiko, A.E. Rautbort, V.M. Tatarintsev, V.M. Filatova, Izv. Akad. Nauk. SSSR, Neorg. Mater. 12 (1976) 273.
[6] R.P. Ingel, D. Lewis III, J. Am. Ceram. Soc. 69 (1986) 325.
[7] M. Yashima, N. Ishizawa, M. Yoshimura, J. Am. Ceram. Soc. 75 (1992) 1541.
[8] V.B. Glushkova, F. Hanic, L.V. Sazonova, Ceramurgia Int. 4 (1978) 176.
[9] R.D. Shannon, Acta Crystallogr. A32 (1976) 751.
[10] E.C. Subbarao, P.H. Sutter, J. Hrizo, J. Am. Ceram. Soc. 48 (1965) 443.
[11] M. Pechini, US Patent 3,330,697 (July 11, 1967).
[12] I.C. Cosentino, PhD Thesis, IPEN-USP, S. Paulo, Brazil, 1997 (in Portuguese).
[13] I.C. Cosentino, R. Muccillo, Mater. Lett. 32 (1997) 295.
[14] H. Otobe, A. Nakamura, Lattice parameters and defect structure of the fluorite and C-type oxide solid solutions between MO_2 and M_2O_3, in: S.C. Singhal, M. Dokiya (Eds.), Proceedings of the Sixth Int. Symp. on Solid Oxide Fuel Cells, The Electrochemical Society, 1999, 463.